

# Parity Relation Based Fault Detection, Isolation and Reconfiguration for Autonomous Ground Vehicle Localization Sensors

Ying Lu, Emmanuel G. Collins, Jr., Majura F. Selekwa  
Department of Mechanical Engineering, FAMU-FSU College of Engineering,  
2525 Pottsdamer Street, Tallahassee, FL 32310  
Email: ying@eng.fsu.edu, ecollins@eng.fsu.edu, majura@eng.fsu.edu

October 6, 2004

## Abstract

This paper considers fault detection, isolation and reconfiguration (FDIR) for the localization sensors, including the dead reckoning and external sensors, of an autonomous ground vehicle (AGV) designed for use in highly unstructured outdoor environments. Ten sensors are considered in this research. None of these sensors are identical, but subsets of them do have the ability to measure or calculate (based on simple algebra) the same kinematical parameters. To improve the localization accuracy, selected sensor outputs are fused using Kalman filters. The fused data and selected sensor measurements are then combined into a set of linearly independent parity equations, which leads to the generation of a bank of residuals. A fault in any one of the ten sensors causes a unique subset of these residuals to grow, which allows the fault to be detected and isolated. This allows a control scheme based on these sensors to reconfigure itself so that only the non-faulty sensors are used for localization. The effectiveness of this FDIR scheme is demonstrated in the context of a recently developed algorithm for maneuvering an AGV in cluttered environments.

**Keywords:** *Fault Detection and Isolation, Fault Reconfiguration, Parity Equations, Localization, Kalman Filter.*

## 1 Introduction

A growing number of research groups around the world are developing autonomous vehicle systems for various applications (see [7,8] for example). More and more attention has been paid to the issue of failure and integrity in navigation systems of vehicles based on sensor technologies [2,3,13]. Many commercial industries have successfully made use of such technology in well-structured environments such as manufacturing and in semi-structured environments such as automated agriculture. The research here focuses on fault detection, isolation and reconfiguration (FDIR) for the localization sensors of wheeled autonomous ground vehicles (AGVs), such as the eXperimental Unmanned Vehicle (XUV) that are designed to operate in highly unstructured outdoor environments. A variety of localization sensors may be used with such vehicles. The experimental platform used here is the ATRV-Jr. [1], shown in Figure 1. Based primarily on the sensors available on the XUV, ten localization sensors are considered. None of these sensors is identical; they each have their own strengths, weaknesses and fault modes. However subsets of these sensors

do have the ability to measure or calculate (based on simple algebra) the same kinematical parameters. The FDIR technique developed here exploits this complex redundancy.

The focus of this paper is on the integration of Kalman filter based sensor fusion and a parity equation based FDIR scheme. In position and orientation estimation, conventional methods, such as odometry, which have been widely used for autonomous vehicles, utilize pulses from wheel encoders to calculate the vehicle's current location. This method is simple and effective. But there exist accumulated errors caused by wheel slippage and therefore the robot may lose track of its location over long distances. To eliminate the drawback of this odometry method in position and orientation estimation, several approaches [4, 9, 10, 14] have been proposed in the past few years. A very good overview is given in [4] with the focus on the 3D location technique using active beacon positioning and the method based on maps and world models. However, many of these results do not use the localization sensors considered here. The research

Report Documentation Page				Form Approved OMB No. 0704-0188	
Public reporting burden for the collection of information is estimated to average 1 hour per response, including the time for reviewing instructions, searching existing data sources, gathering and maintaining the data needed, and completing and reviewing the collection of information. Send comments regarding this burden estimate or any other aspect of this collection of information, including suggestions for reducing this burden, to Washington Headquarters Services, Directorate for Information Operations and Reports, 1215 Jefferson Davis Highway, Suite 1204, Arlington VA 22202-4302. Respondents should be aware that notwithstanding any other provision of law, no person shall be subject to a penalty for failing to comply with a collection of information if it does not display a currently valid OMB control number.					
1. REPORT DATE <b>00 DEC 2004</b>		2. REPORT TYPE <b>N/A</b>		3. DATES COVERED <b>-</b>	
4. TITLE AND SUBTITLE <b>Parity Relation Based Fault Detection, Isolation and Reconfiguration for Autonomous Ground Vehicle Localization Sensors</b>				5a. CONTRACT NUMBER	
				5b. GRANT NUMBER	
				5c. PROGRAM ELEMENT NUMBER	
6. AUTHOR(S)				5d. PROJECT NUMBER	
				5e. TASK NUMBER	
				5f. WORK UNIT NUMBER	
7. PERFORMING ORGANIZATION NAME(S) AND ADDRESS(ES) <b>Department of Mechanical Engineering, FAMU-FSU College of Engineering, 2525 Pottsdamer Street, Tallahassee, FL 32310</b>				8. PERFORMING ORGANIZATION REPORT NUMBER	
9. SPONSORING/MONITORING AGENCY NAME(S) AND ADDRESS(ES)				10. SPONSOR/MONITOR'S ACRONYM(S)	
				11. SPONSOR/MONITOR'S REPORT NUMBER(S)	
12. DISTRIBUTION/AVAILABILITY STATEMENT <b>Approved for public release, distribution unlimited</b>					
13. SUPPLEMENTARY NOTES <b>See also ADM001736, Proceedings for the Army Science Conference (24th) Held on 29 November - 2 December 2005 in Orlando, Florida. , The original document contains color images.</b>					
14. ABSTRACT					
15. SUBJECT TERMS					
16. SECURITY CLASSIFICATION OF:			17. LIMITATION OF ABSTRACT <b>UU</b>	18. NUMBER OF PAGES <b>8</b>	19a. NAME OF RESPONSIBLE PERSON
a. REPORT <b>unclassified</b>	b. ABSTRACT <b>unclassified</b>	c. THIS PAGE <b>unclassified</b>			

in [9] and [10] does use similar sensors. In particular, a magnetic compass is used in [9] to calibrate the orientation drift error caused by wheel slippage, thereby resulting in robot position recovery. It is based on a series of experiments. The research reported in [10] developed a method named the UMBmark for quantitatively measuring systematic odometry errors and, to a limited degree, nonsystematic errors. The calculation of all the odometry errors terms is time-consuming and therefore lacks flexibility.

The research in [14] uses Kalman filter to improve the accuracy of mobile robot localization. Kalman filtering is adopted for fusing information from an electronic compass and wheel encoders. This method is simple and effective. As in [14], the research in this paper develops a bank of Kalman filters to provide more accurate localization for FDIR based on a simplified kinematical model of the robot. The fused outputs of the Kalman filters and selected sensor measurements are then combined into a set of linearly independent parity equations, which leads to the generation of a bank of residuals. A fault in any one of the ten sensors causes a unique subset of these residuals to grow, which allows the fault to be detected and isolated. This allows a control scheme based on these sensors to reconfigure itself so that only the non-faulty sensors are used for localization. The effectiveness of this FDIR scheme is demonstrated in the context of a recently developed algorithm for maneuvering an AGV in cluttered environments.

The research developed here provides an almost complete automated FDIR system for the localization sensors. However, it does not yet include the integration of DGPS or GPS. The integration of DGPS or GPS with the inertial navigation system and the means of detection in DGPS or GPS are planned for future research.

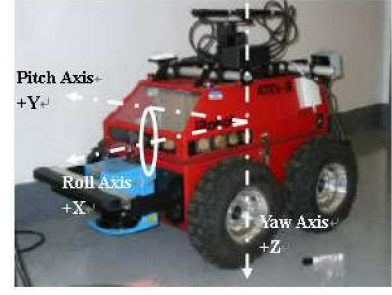


Figure 1: The ATRV-Jr. with its Body Frame

This paper is organized as follows. Section 2 describes the ATRV-Jr. localization sensors information and potential sensor fault sources. Then it presents the respective kinematical equations for vehicle position, attitude and velocity. Section 3 overviews the FDIR procedures with the focus on the fault residuals and the truth table which shows how a fault in any one of the sensors causes a unique combination of residuals to grow. Section 4 presents computer simulation results that demonstrate the accuracy of the FDIR scheme by navigating an ATRV-Jr. robot in an environment crowded with obstacles. The navigation algorithm realizes goal seeking and obstacle avoidance behaviors, the former of which is based on the related localization sensor measurements.

## 2 Localization Sensors and Potential Faults

The ATRV-Jr. (shown in Figure 1) is an all-terrain robotic research platform capable of autonomous operation [1]. Localization information is critical for the purpose of navigation and guidance of the autonomous vehicle. The localization sensor suite consists of two wheel encoders, one fluxgate compass including a tilt sensor, one electrical compass including a tilt sensor, one non-contact Doppler sensor, one DGPS, one inertial navigation system, which includes three accelerometers and three gyroscopes. Table 1 lists each sensor and the information it provides and standard fault sources. For example, the accumulated errors caused by wheel slippage is the typical fault source of the wheel encoders.

Sensors	Measured Quantity	Standard Fault Sources
Wheel encoder	Velocity	Wheel slippage
Fluxgate compass Tilt sensor in Fluxgate compass	Orientation angle Pitch and roll angle	Disturbance by other magnetic field and inclination
Electrical compass Tilt sensor in Electrical compass	Orientation angle Pitch and roll angle	High voltage wires, large metal structures and inclination
Doppler sensor	Velocity	Strength of the return signal, field of the view
Longitudinal accelerometer Lateral accelerometer Yaw angle rate sensor Pitch angle rate sensor Roll angle rate sensor	Longitudinal acceleration Lateral acceleration Yaw angle rate Pitch angle rate Roll angle rate	Bias and misalignment of the unit's axes

Table 1: Localization Sensor Set and Fault Sources

### 3 Parity Relation Based FDIR Scheme

This research uses the FDIR scheme based on parity relations combined with the fused data and selected sensor measurements. A bank of residuals using these parity relations is then generated. A fault in any one of the ten sensors causes a unique subset of these residuals to grow, which allows the fault to be detected and isolated.

#### 3.1 Parity Relations Based on Position and Orientation

Integrating multiple sensors into the process is time efficient and can provide more reliable sensing information. It therefore improves the reliability of the system. The Kalman filter is used in this research for fusing sensor outputs from the compasses with the odometry estimates employing wheel encoders. Kalman Filtering [11, 12] is a well known technique for state and parameter estimation. There are two compasses used in this project; one is a fluxgate compass and the other is an electrical compass. They are added to overcome the wheel slippage problem related to the odometry method. In the fusion algorithm, the wheel encoders propagate the trajectory state vector made up of longitudinal and lateral position and orientation. The two compasses provide redundant orientation measurements, which the filter uses to calculate corrections to the trajectory state and estimate the wheel encoder sensor errors.

##### 3.1.1 Longitudinal and Lateral Position

Assuming knowledge of the initial position, the longitudinal and lateral position of the vehicle can be obtained by three different methods:

1. Fusion of the wheel encoders and fluxgate compass using a Kalman filter

2. Fusion of the wheel encoders and fluxgate compass using a Kalman filter
3. Integration of the longitudinal or lateral acceleration from the Inertial Navigation System(INS)

The kinematical model which is used by the two Kalman filters is as follows:

$$x_{k+1} = x_k + T(v_{tot} \sin \theta_{k+1}), \quad (1)$$

$$y_{k+1} = y_k - T(v_{tot} \cos \theta_{k+1}), \quad (2)$$

$$\theta_{k+1} = \theta_k - T\dot{\theta}, \quad (3)$$

$$\dot{\theta} = \frac{v_R - v_L}{l}, \quad (4)$$

$$v_{tot} = \frac{v_R + v_L}{2}. \quad (5)$$

where  $x$  denotes the lateral displacement,  $y$  denotes the longitudinal displacement,  $\theta$  is the orientation angle,  $\dot{\theta}$  is the yaw rate,  $v_{tot}$  is the velocity of the center of the vehicle,  $v_R$  and  $v_L$  are the direct outputs of the right and left wheel encoders,  $l$  ( $= 0.55m$ ) denotes the distance between the two drive wheels and  $T$  stands for the sampling period. It is well known that heading errors cause large lateral position errors, which increase proportionally with the distance travelled by the vehicle. Orientation compasses, which include a fluxgate compass and an electrical compass, can be applied to measure the orientation of the vehicle and fuse respectively with the orientation angle estimated by the wheel encoders to overcome the problem of accumulation of errors.

The INS includes three accelerometers and three gyroscopes. They provide the acceleration, pitch, roll and yaw angular rate information respectively, in the body frame (Figure 1). The longitudinal and lateral accelerometers in the INS are used for velocity and position information. Integrating the direct outputs from the two accelerometers twice provides the needed position information. Pitch, roll and yaw angle rate information are provided by the three gyroscopes. The errors caused by bias in the sensor readings accumulate with time and inaccurate readings are caused by

the misalignment of the unit's body frame with respect to the local navigation frame.

Here we define  $z_0$  as the direct output of the left wheel encoder,  $z_1$  and  $z_4$  as the fused longitudinal and lateral information from two wheel encoders and fluxgate compass respectively,  $z_2$  and  $z_5$  as the fused longitudinal and lateral information from two wheel encoders and electrical compass respectively,  $z_3$  and  $z_6$  as the integrated data from longitudinal and lateral accelerometers in the INS respectively. Equations (6) and (7) show that the right and left velocities may be calculated respectively as:

$$\hat{v}_L = v_{tot} - \frac{l}{2}\dot{\theta}, \quad (6)$$

$$\hat{v}_R = v_{tot} + \frac{l}{2}\dot{\theta}. \quad (7)$$

where  $\hat{v}_L$  and  $\hat{v}_R$  denote the calculated left and right wheel encoder values respectively. By comparing the calculated values to the real outputs from both the encoders it is possible to identify which one is at fault. The following four residuals based on parity equations between the outputs of the two Kalman filters and the INS are calculated by using different combinations of the above longitudinal and lateral position signals:

$$r_0 = z_0 - \hat{v}_R, \quad (8)$$

$$r_1 = \max(|z_1 - z_2|, |z_4 - z_5|), \quad (9)$$

$$r_2 = \max(|z_1 - z_3|, |z_4 - z_6|), \quad (10)$$

$$r_3 = \max(|z_2 - z_3|, |z_5 - z_6|). \quad (11)$$

Table 2 can then be used to detect a fault in any one of the position sensor or sensor groups.

Fault Sensor	$r_0$	$r_1$	$r_2$	$r_3$
Left Wheel Encoders	H	H	H	H
Right Wheel Encoders	L	H	H	H
Fluxgate Compass	L	H	H	L
Electrical Compass	L	H	L	H
INS	L	L	H	H

Table 2: Truth Table for Wheel Encoder Fault Detection

### 3.1.2 Vehicle Orientation

The orientation of the vehicle can be obtained by three different methods:

1. Fusion of the wheel encoders and the fluxgate compass based on a Kalman filter
2. Fusion of the wheel encoders and the electrical compass based on a Kalman filter

3. Integration of the Yaw angle rate sensor information in the INS

The kinematic equations which are the basis of the Kalman filter used in the second method are Equations (1)-(3).

The following three residuals based on parity equations between the outputs of the multiple Kalman filters and yaw angle rate sensor are calculated by using different combinations of the above orientation signals:

$$r_4 = z_7 - z_8, \quad (12)$$

$$r_5 = z_7 - z_9, \quad (13)$$

$$r_6 = z_8 - z_9. \quad (14)$$

Where  $z_7$  denotes the fused orientation information from two wheel encoders and the fluxgate compass,  $z_8$  is the fused orientation information from two wheel encoders and the electrical compass and  $z_9$  is the integrated data from the yaw angle rate sensor in the INS. Table 3 can then be used to detect a fault in any one of the three orientation sensors.

Faulty Sensor	$r_4$	$r_5$	$r_6$
Fluxgate Compass	H	H	L
Electrical Compass	H	L	H
Gyroscope	L	H	H

Table 3: Truth Table for Orientation Sensor Fault Detection

## 3.2 Parity Relations Based on Velocity

Here the velocity denotes the velocity of the center of the robot and is based on a 3-axis coordinate frame aligned along the vehicle body (see Figure 1). The maximum velocity is 1 m/s.

### 3.2.1 Vehicle Velocity

The velocity of the vehicle can be obtained by three different methods as follows:

1. The two wheel encoders using (5)
2. Integration of the longitudinal accelerometer information in the INS
3. The Doppler sensor

In the third method, the Doppler non-contact speed measurement using the Delta speed sensor is achieved through the use of Doppler radar.

The following three residuals are therefore used as the bases for the velocity parity relations:

$$r_7 = z_{10} - z_{11}, \quad (15)$$

$$r_8 = z_{10} - z_{12}, \quad (16)$$

$$r_9 = z_{11} - z_{12}, \quad (17)$$

where  $z_{10}$  is the velocity determined from the two wheel encoders,  $z_{11}$  is the velocity obtained by integrating the data from longitudinal accelerometer in the INS, and  $z_{12}$  is the velocity determined by the Doppler sensor. Table 4 can then be used to detect a fault in any one of the three velocity sensors or sensor groups.

Faulty Sensor	$r_7$	$r_8$	$r_9$
Wheel Encoders	H	H	L
INS	H	L	H
Doppler Sensor	L	H	H

Table 4: Truth Table for Velocity Sensor Fault Detection

### 3.3 Parity Relations Based on Attitude Sensors

Attitude denotes the roll and pitch angles of the vehicle. Here the attitude is aligned with the 3-axis body coordinates (see Figure 1). Three groups of sensors supply attitude measurements: the INS, the fluxgate compass and the electrical compass. Both compasses measure roll and pitch angles in the range of degrees [-45 45].

#### 3.3.1 Vehicle Pitch Angle

The pitch angle of the vehicle can be obtained by three different methods as described follows:

1. Integration of the pitch angle rate sensor information in the INS
2. Pitch output from the fluxgate compass
3. Pitch output from the electrical compass

The following three residuals are the bases for velocity parity equations among the outputs of the above pitch angle signals:

$$r_{10} = z_{13} - z_{14}, \quad (18)$$

$$r_{11} = z_{13} - z_{15}, \quad (19)$$

$$r_{12} = z_{14} - z_{15}, \quad (20)$$

Where  $z_{13}$  denotes the integrated data from pitch angle rate sensor in INS,  $z_{14}$  is the pitch output from fluxgate compass and  $z_{15}$  is the pitch output from electrical compass. Table 5 can then be used to detect a fault in any one of the three pitch angle sensors.

Faulty Sensor	$r_{10}$	$r_{11}$	$r_{12}$
Pitch Gyroscope	H	H	L
Fluxgate Compass	H	L	H
Electrical Compass	L	H	H

Table 5: Truth Table for Pitch Attitude Sensor Fault Detection

#### 3.3.2 Vehicle Roll Angle

Table 6 can then be used to detect a fault in any one of the three roll angle sensors using the same method.

Faulty Sensor	$r_{13}$	$r_{14}$	$r_{15}$
Roll Gyroscope	H	H	L
Fluxgate Compass	H	L	H
Electrical Compass	L	H	H

Table 6: Truth Table for Roll Attitude Sensor Fault Detection

## 4 A System for Automated Fault Detection and Isolation

Table 7 summarizes 18 different output signals used in the vehicle navigation system. Some are directly measured, while the others are fused using Kalman filters. Table 8 summarizes 15 different residuals calculated using combinations of the output signals from Table 7. It includes longitudinal and lateral position, orientation, longitudinal velocity and attitude information.

By processing the above 15 different residuals, it is possible to identify a fault in any of the sensors. Table 9 shows how a fault in any one of the sensors causes a unique combination of residuals to grow. The corresponding faulty sensor can then be detected and identified.



Output	Description	Sensors Related
$z_1$	Robot	Wheel encoders, fluxgate compass
$z_2$	longitudinal	Wheel encoders, electrical compass
$z_3$	position	Longitudinal accelerometer in INS
$z_4$	Robot	Wheel encoders, fluxgate compass
$z_5$	lateral	Wheel encoders, electrical compass
$z_6$	position	Lateral accelerometer in INS
$z_7$	Robot	Wheel encoders, fluxgate compass
$z_8$	heading	Wheel encoders, electrical compass
$z_9$	angle	Yaw angle rate sensor in INS
$z_{10}$	Robot	Wheel encoders
$z_{11}$	longitudinal	Longitudinal accelerometer in INS
$z_{12}$	velocity	Non-contact Doppler sensor
$z_{13}$	Robot	Pitch angle rate sensor in INS
$z_{14}$	pitch	Fluxgate compass
$z_{15}$	attitude	Electrical compass
$z_{16}$	Robot	Roll angle rate sensor in INS
$z_{17}$	roll	Fluxgate compass
$z_{18}$	attitude	Electrical compass

Table 7: Bank of Signals for Fault Detection and Identification Scheme

## 5 Simulation Results

The fault detection and identification scheme designed in the previous sections was simulated to test its performance. We apply it to navigation of the ATRV-Jr. in a dense forest using a multivalued fuzzy behavior control algorithm [6]. The algorithm realizes goal seeking, and obstacle avoidance functions. The goal seeking behavior directs the robot to a specific predefined target. The objective of the goal seeking behavior is to make the difference between the robot heading direction and the goal direction as small as possible. The obstacle avoidance behavior for the velocity control activity uses the minimum distance to the nearest obstacle and the current velocity to determine the amount by which the velocities of the two wheels should be changed. When the robot has some localization sensors at fault, the FDIR scheme can detect the faulty sensors and reconfigure the control sys-

tem so that it uses only non-faulty sensors.

For the simulation, the assumed sensor measurement noises were Gaussian white noise. The ATRV-Jr was assumed to be travelling with the velocity of the right and left wheels around 0.53m/s respectively with the roll and pitch angles in the range of degrees  $[-45,45]$ .

### 5.1 Longitudinal Position Sensor Fault Detection

As described in Subsection 3.2.1, there are three sensor groups that can be fused using Kalman filters to provide longitudinal position data for the vehicle navigation system. In the simulation, the default method for position information is the third method, that is, double integration of the longitudinal accelerometer outputs from the INS. While a fault in the sensor is detected, the scheme will switch to the reconfiguration step. In the simulation, a fault in the longitudinal accelerometer was said to occur at  $t = 14s$ , which caused two longitudinal residuals among the three to be big enough to identify the fault. When there was no FDIR scheme, the faulty sensor outputs were used continuously. The forest navigation algorithm then operated based on faulty information, which caused the robot to fail to fulfill both obstacle avoidance and goal seeking.

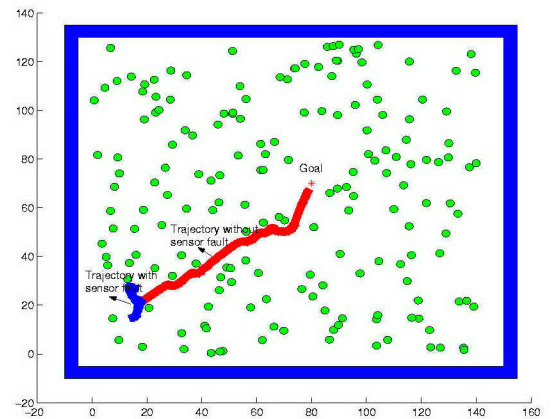


Figure 2: Trajectories with and without INS Sensor Fault

Figure 2 shows the normal trajectory and the faulty trajectory with longitudinal accelerometer fault occurring at  $t = 14s$  without FDIR scheme. It is shown that when there is no any fault occurs, the algorithm works well and the robot can avoid the trees and arrive at the desired destination. When the default position sensor fault occurs from the 14 second without detection, the robot hits one or more trees in about 4 sec and stop and therefore lose track of the goal. Figure 3 presents a comparison of the two trajectories with and without the FDIR. With FDIR, the faulty accelerometer can be detected and replaced with fused position data from

Faulty Sensor	$r_1$	$r_2$	$r_3$	$r_4$	$r_5$	$r_6$	$r_7$	$r_8$	$r_9$	$r_{10}$	$r_{11}$	$r_{12}$	$r_{13}$	$r_{14}$	$r_{15}$
Wheel Encoders	H	H	H	H	H	H	H	H	L	L	L	L	L	L	L
Fluxgate heading compass	H	H	L	H	H	L	L	L	L	H	L	H	H	L	H
Electrical heading compass	H	L	H	H	L	H	L	L	L	L	H	H	L	H	H
Lateral accelerometer	L	H	H	L	L	L	L	L	L	L	L	L	L	L	L
Longitudinal accelerometer	L	H	H	L	L	L	H	L	H	L	L	L	L	L	L
Yaw angle rate sensor	L	L	L	L	H	H	L	L	L	L	L	L	L	L	L
Non-contact Doppler sensor	L	L	L	L	L	L	L	H	H	L	L	L	L	L	L
Pitch angle rate sensor	L	L	L	L	L	L	L	L	L	H	H	L	L	L	L
Roll angle rate sensor	L	L	L	L	L	L	L	L	L	L	L	L	H	H	L

Table 9: Complete Truth Table for Navigation Sensor Fault Detection

the fluxgate compass and the wheel encoders. The re-configuration allows the robot to avoid the trees and

achieve its goal.

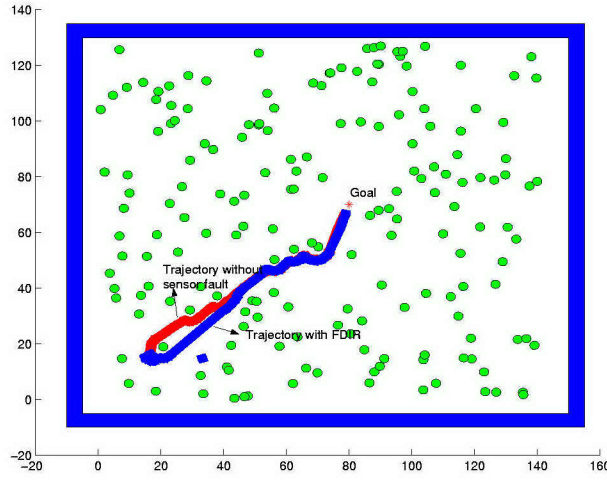


Figure 3: Trajectories with and without Position FDIR with INS Sensor Fault

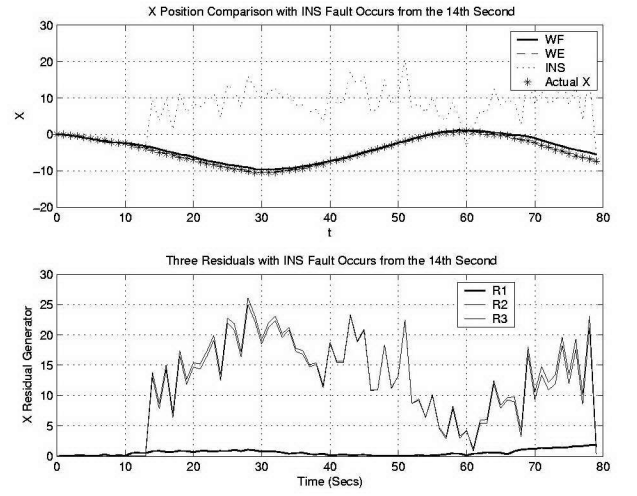


Figure 4: Longitudinal Position Outputs and Three Residual Comparisons with INS Fault

Figure 4 shows the comparison of the longitudinal position outputs from the three different methods and the values of the residuals  $r_1$ ,  $r_2$  and  $r_3$  respectively with the longitudinal accelerometer fault occurrence from the 14th second (see Table 2). It is clearly seen that fused outputs from the two Kalman filters are similar to each other while the outputs from the INS is different from the two others from the 14th second. Correspondingly, only residue  $r_1$  is low which indicates that the sensor in the INS is at fault and the faulty sensor is detected and identified.

The simulation results for lateral position and orientation sensor FDIR were also obtained. They are similar to that of the longitudinal position sensor FDIR.

## 5.2 Velocity Sensor Fault Detection

Three groups of sensors provide velocity information for the measurement of the dynamic motion of the robot as described in Subsection 3.2.1. When no velocity sensor fault occurs, the second method is the default approach, that is integrating the output once from the longitudinal accelerometer in the INS. Figure 5 shows the situation when the default INS sensor is at fault from the 14th sec. The robot cannot avoid the obstacles. It hits the tree and stops in about 4 sec and will not successfully arrive at the destination without FDIR. While with the fault detection and identification, the faulty sensor output will be replaced by the Doppler sensor for the velocity information. It is seen that the robot can avoid the obstacle and thereafter reach the destination Figure 6 shows the comparison of three velocity outputs and the values of three residuals  $r_7$ ,  $r_8$  and  $r_9$  of Table 4 during the INS sensor fault. It is clear that only residue  $r_8$  is low which in-



icates that the INS sensor is the faulty component.

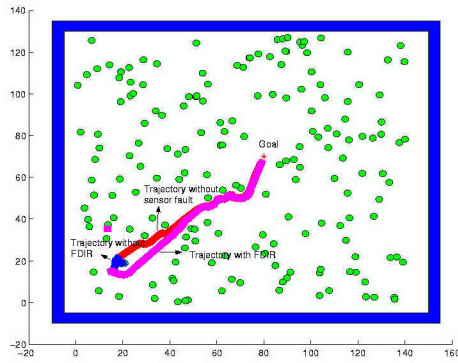


Figure 5: Trajectories with and without Velocity FDIR with the INS Fault

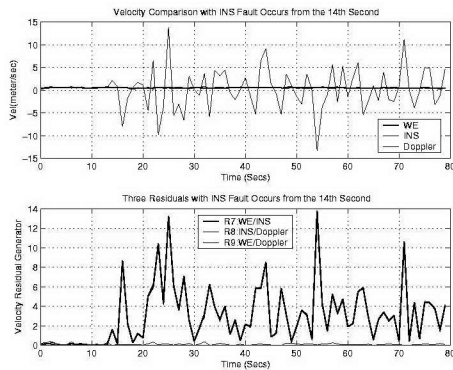


Figure 6: Velocity Outputs and Three Residual Comparisons with INS Fault

## 6 Conclusion

This paper develops an effective parity equation based fault detection and identification system providing a methodology to continuously monitor all the sensors used in the vehicle navigation to ensure the system health, excluding Differential GPS. Meantime the Kalman filter based fusion method provides more reliable information. The scheme was shown to work well when simulated with our detailed research robot model. Experimental implementation of the entire fault detection and identification system on the ATRV-Jr. is expected to occur in the near future.

## References

- [1] ATRV-Jr All-Terrain Mobile Robot User's Guide, iRobot Corp., Somerville, MA, 2001.
- [2] R. Isermann, *Supervision, Fault-Detection and Fault-Diagnosis Methods - An Introduction*, Control Eng. Practice, Vol.5, No.5, pp. 639-652, March 1997.
- [3] Rajesh Rajamani, Adam S. Howell, Chieh Chen, J. Karl Hedrick and Masayoshi Tomizuka, *A Complete Fault Diagnostic System for Automated Vehicles Operating in a Platoon*, IEEE Transactions on Control Systems Technology, Vol. 9, No. 4, pp. 553-564, July 2001.
- [4] Jason Gu and Max Meng, *Sensor Fusion in Mobile Robot: Some Perspectives*, Proceedings of the 4th World Congress on Intelligent Control and Automation, pp.1194-1199, Shanghai, P.R.China., June 10-14, 2002.
- [5] Olle Wijk and Patric Jensfelt, *Sensor Fusion for Mobile Robot Navigation-A First Subjective Discussion*, Centre of Autonomous System at KTH, Mar 27, 1997.
- [6] Majura F. Seleka and Emmanuel G. Collins, Jr., *Centralized Fuzzy Behavior Control for Robot Navigation*, Proceedings of the 2003 IEEE International Symposium on Intelligent Control Houston, Texas, October 5-8, 2003.
- [7] J. Borenstein, H. R. Everett, L. Feng and D. Wehe, *Mobile Robot Positioning Sensors and Techniques*, J. Robot. Syst., vol 14, no. 4, pp. 231-249, 1997.
- [8] R. Chatila, S. Lacroix, S. Betge-Brezetz, M. Devy and T. Simeon, *Autonomous Mobile Robot Navigation for Planet Exploration-The EDEN Project*, Proc. IEEE Int. Conf. Robot. Automat., 1996.
- [9] J. Borenstein, Liqiang Feng, *Correction of Systematic Odometry Errors in Mobile Robots*, Proceedings of the 1995 International Conference on Intelligent Robots and Systems (IROS '95), Pittsburgh, Pennsylvania, pp. 569-574, August 5-9, 1995.
- [10] Borenstein. J. & Feng, L. *Measurement and Correction of Systematic Odometry Errors in Mobile Robot*, IEEE Trans. On Rob. And Autom., 126pp. 869-880, 1996.
- [11] R.E.Kalman, *A new Approach to Linear Filtering and Prediction Problems*, ASME Journal of Basic Engineering, 86:35-45, 1960.
- [12] P. S. Maybeck, *Stochastic Models, Estimation and Control*, Vo. 1. New York: Academic Press, 1979.
- [13] Stergios I. Roumeliotis, Gaurav S. Sukhatme and George A. Bekey, *Fault Detection and Identification in a Mobile Robot using Multiple-Model Estimation*, IEEE International Conference on Robotics and Automation, Leuven, Belgium, pp. 2223-2228, May 16-21, 1998.
- [14] Kai-Tai Song, Yuon-Hau Chen, *Development of Multiple Sensor Fusion Experiments for Mechatronics Education*, Proc. Natl. Sci. Coun. Roc(D), Vo. 9, No. 2, pp. 56-64, 1999.